# Multiple quantum NMR and relaxation of an oriented $CH_3$ group

J. Tang and A. Pines

*University of California, Berkeley, California 94720*
(Received 11 October 1979; accepted 19 November 1979)

NMR relaxation of the $n$-quantum transitions ($n = 1,2,3$) for an oriented $CH_3$ group by paramagnetic impurities is discussed. The $n$-quantum spectra are presented, and the effect of the correlation of fluctuations in random fields at the three proton sites on symmetry-breaking relaxation transitions is outlined. Experimental results on acetonitrile dissolved in liquid crystalline EBBA with paramagnetic DTBN are presented together with a discussion on correlations of fluctuation and correlation times.

## I. INTRODUCTION

The applicability of NMR as a spectroscopic tool has been greatly enhanced by the recent advent of multiple quantum spectroscopy.[1-8] This allows the observation of normally forbidden $n$-quantum transitions in coupled spin systems. As an example, the $n = 0, 1, \ldots, 6$ spectra of the six-proton group in oriented benzene were produced,[5,6] exhibiting the expected simplification of spectra as $n$ gets larger. This allows an easy analysis of the spectra (where the normal one-quantum spectrum may be intractable) and straightforward structural assignment of dipolar splittings without the need for isotopic (spin) labeling. The highest order ($N$-quantum) transition is completely independent of the couplings and this has been used to measure chemical shifts for quadrupolar spins in solids by double quantum NMR.[3] Other aspects have included double quantum spin locking and double quantum cross polarization.[3]

A particularly interesting feature of multiple quantum NMR is the information available from the $n$-quantum relaxation. Stoll *et al.*[4] have shown that relaxation of the forbidden double quantum transition in two spin AX spin system contains information on the correlated fluctuations at the A and X sites. In a thorough discussion, Wokaun and Ernst also presented the theory for $n$-quantum relaxation and showed experimental results on a two-spin system in an isotropic fluid.[7] Further, Poupko *et al.* and Bodenhausen *et al.* have demonstrated the applicability of multiple quantum NMR to the study of relaxation and motion in coupled systems of deuterium nuclear spins.[8]

We have been interested in the multiple quantum NMR of strongly dipolar coupled spin-$1/2$ nuclei in oriented systems (solids, liquid crystals). These illustrate the behavior of systems with high symmetry, for example a $CH_3$ group or benzene. Normally, radiofrequency irradiation can induce only transitions between eigenstates belonging to the same irreducible representations of the spin Hamiltonian. However, relaxation by fluctuating random fields may induce symmetry-breaking transitions and the study of $n$-quantum spectra and their relaxation should allow a complete determination of the fluctuations, correlations, and symmetry-breaking pathways. This provides a useful tool in addition to the elegant selective excitation and normal mode relaxation techniques in one-quantum spectroscopy described by Werbelow and Grant.[9] In this paper we present a first study of the relaxation of dipolar coupled three-proton system ($CH_3$ group) by paramagnetic impurities in a liquid crystal solvent. The one-, two-, and three-quantum linewidths were studied over a wide concentration range and the accurate linewidth ratios allowed a determination of the fact that fluctuations are correlated and a measurement of the correlation times.

Section II describes the $n$-quantum spectra of a dipolar coupled $CH_3$ group and Sec. III provides a concise theory of $n$-quantum relaxation for this symmetry group. Experimental results and discussion are presented in Sec. IV.

## II. MULTIPLE QUANTUM SPECTRA OF METHYL GROUP

The NMR spectrum of an oriented solute in a liquid crystal is generally dominated by dipolar structure. It is due to the incomplete motional averaging out of the intramolecular dipolar interactions. The methyl protons of acetonitrile, for example, have $C_3$ symmetry with symmetry axis perpendicular to the proton plane. The eigenstates can be classified by their symmetry characteristics and contain one quartet and two doublets.[11] The observable multiple quantum transitions are those transitions connecting the states of the same irreducible representation. The energy diagram and the possible multiple quantum transitions are shown in Fig. 1. The eigenstates are given by

$$|1\rangle = |A_{3/2}\rangle = |\uparrow\uparrow\uparrow\rangle \ ,$$

$$|2\rangle = |A_{1/2}\rangle = \frac{1}{\sqrt{3}}\left(|\uparrow\uparrow\downarrow\rangle + |\uparrow\downarrow\uparrow\rangle + |\downarrow\uparrow\uparrow\rangle\right) \ ,$$

$$|3\rangle = |A_{-1/2}\rangle = \frac{1}{\sqrt{3}}\left(|\downarrow\downarrow\uparrow\rangle + |\downarrow\uparrow\downarrow\rangle + |\uparrow\downarrow\downarrow\rangle\right) \ ,$$

$$|4\rangle = |A_{-3/2}\rangle = |\downarrow\downarrow\downarrow\rangle \ ,$$

$$|5\rangle = |E^a_{1/2}\rangle = \frac{1}{\sqrt{3}}\left(|\uparrow\uparrow\downarrow\rangle + \epsilon|\uparrow\downarrow\uparrow\rangle + \epsilon^*|\downarrow\uparrow\uparrow\rangle\right) \ ,$$

$$|6\rangle = |E^a_{-1/2}\rangle = \frac{1}{\sqrt{3}}\left(|\downarrow\downarrow\uparrow\rangle + \epsilon|\downarrow\uparrow\downarrow\rangle + \epsilon^*|\uparrow\downarrow\downarrow\rangle\right) \ ,$$

$$|7\rangle = |E^b_{1/2}\rangle = \frac{1}{\sqrt{3}}\left(|\uparrow\uparrow\downarrow\rangle + \epsilon^*|\uparrow\downarrow\uparrow\rangle + \epsilon|\downarrow\uparrow\uparrow\rangle\right) \ ,$$

$$|8\rangle = |E^b_{-1/2}\rangle = \frac{1}{\sqrt{3}}\left(|\downarrow\downarrow\uparrow\rangle + \epsilon^*|\downarrow\uparrow\downarrow\rangle + \epsilon|\uparrow\downarrow\downarrow\rangle\right) \ ,$$

where $\epsilon = \exp(i2\pi/3)$.

 0021-9606/80/053290-08$01.00 

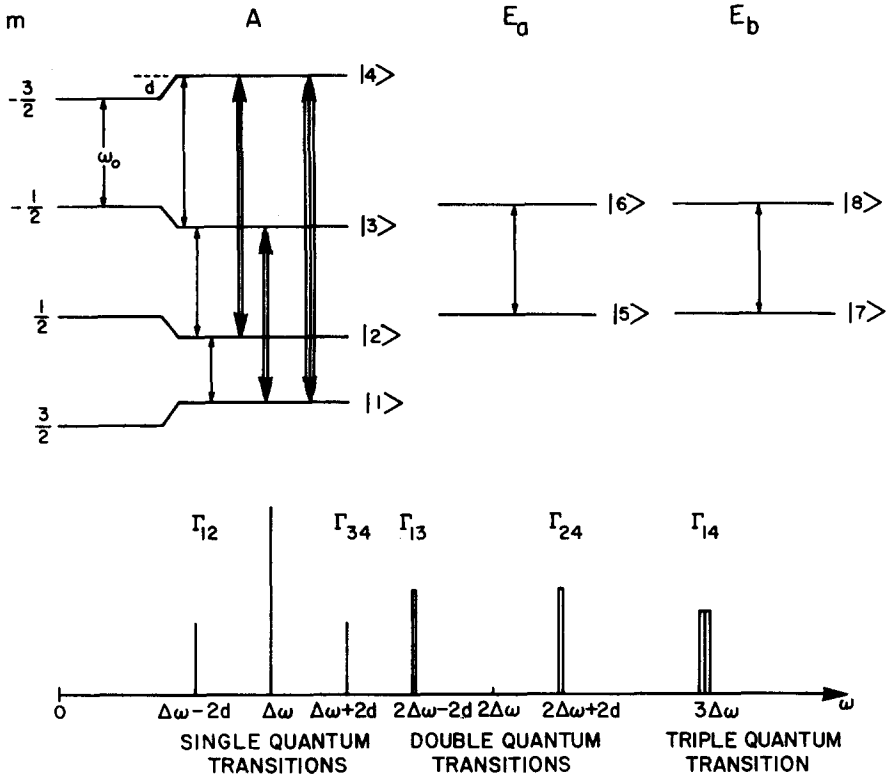


FIG. 1. The energy level diagram of dipolar-coupled methyl protons in a magnetic field. $\Delta\omega$ is the frequency offset in the rotating frame and $d$ is the dipolar shift. The lower half shows a stick spectrum of the multiple quantum transitions. The associated relaxation rates $\Gamma_{ij}$ are related to their linewidths.

The frequencies of the allowed multiple quantum transitions in the rotating frame (resonance offset $\Delta\omega$) are listed in Table I.

The method used to observe the multiple quantum spectra is the TPPI method described in Ref. 6. In this method, the frequency offset $\Delta\omega$ is created artificially by phase increments. A theoretical stick spectrum is shown in Fig. 1. The intensity of each transition depends on the time of preparation period and mixing period of the multiple pulse sequence, dipolar coupling strength and the real frequency offset.

The experimental spectrum shown in Fig. 2 exhibits the expected multiple quantum transitions all separated according to order. Resolution is limited by truncation of the multiple quantum free induction decay. The actual linewidth is less than 5 Hz.

TABLE I. Allowed multiple quantum transitions.

| Transition origin | Frequency | $M$ |
|---|---|---|
| $A_{1/2}-A_{3/2}$ | $\Delta\omega-2d$ | $\Delta M=1$ |
| $A_{-1/2}-A_{1/2}$ | $\Delta\omega$ | Single quantum transition |
| $A_{-3/2}-A_{-1/2}$ | $\Delta\omega+2d$ | |
| $E^a_{-1/2}-E^a_{1/2}$ | $\Delta\omega$ | |
| $E^b_{-1/2}-E^b_{1/2}$ | $\Delta\omega$ | |
| $A_{-1/2}-A_{3/2}$ | $2\Delta\omega-2d$ | $\Delta M=2$ |
| $A_{-3/2}-A_{1/2}$ | $2\Delta\omega+2d$ | Double quantum transition |
| $A_{-3/2}-A_{3/2}$ | $3\Delta\omega$ | $\Delta M=3$ Triple quantum transition |

## III. MULTIPLE QUANTUM RELAXATION THEORY

To specify completely a quantum mechanical system in nonequilibrium, one has to determine the occupation probabilities of the system in each state and the phase relation between each pair of states. A more complete understanding of the population and phase relaxation mechanisms can be obtained by the use of multiple

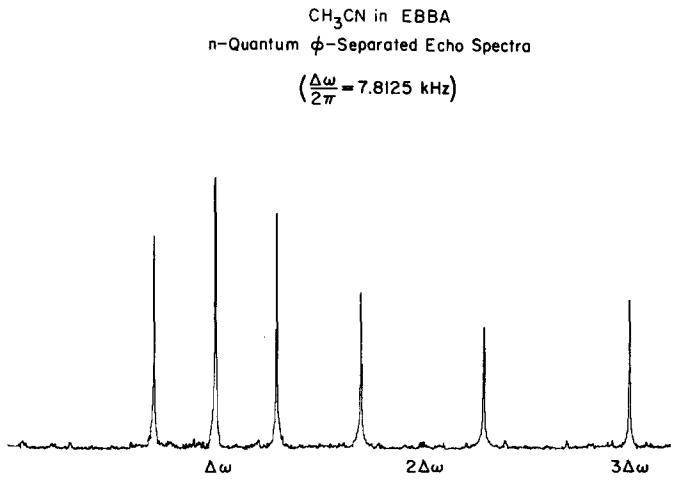


FIG. 2. The multiple quantum spectrum of oriented methyl protons. It consists of three single quantum transitions, two double quantum transitions, and one triple quantum transition. The resolution is limited by truncation of the multiple quantum free induction decay. Inhomogeneous broadening was removed by echoes in the TFPI sequence (Fig. 5).

quantum spectroscopy as shown in detail by Wokaun and Ernst.[7] We outline the relevant aspects of the theory for our case.

### A. Redfield theory

A general approach to study relaxation using the density matrix formalism is that of Redfield.[12] The Hamiltonian of the coupled spin system during the evolution period of multiple quantum coherence can be written as

$$H = H_0 + H_D + H_1(t) \quad . \tag{1}$$

Here $H_0$ is the Zeeman term of the spin system in a strong magnetic field and $H_D$ is the intramolecular dipolar coupling term. The time dependent term $H_1(t)$ describes the fluctuation of the coupling between the spin system and the relaxation agents.

To describe the time of evolution of the multiple quantum coherences, we study the off-diagonal elements of the density matrix. The equation of motion of the phase coherence between states $|\alpha\rangle$ and $|\beta\rangle$ is given by[10]

$$\frac{d}{dt}\rho_{\alpha\beta}(t) = -i\Omega_{\alpha\beta}\rho_{\alpha\beta}(t) - \Gamma_{\alpha\beta}\rho_{\alpha\beta}(t) \quad . \tag{2}$$

Here $\Omega_{\alpha\beta}$ is the transition frequency between states $|\alpha\rangle$ and $|\beta\rangle$. The relaxation rate is given by[13]

$$\Gamma_{\alpha\beta} = \Gamma^{(0)}_{\alpha\beta} + \Gamma'_{\alpha\beta} \quad , \tag{3}$$

where

$$\Gamma^{(0)}_{\alpha\beta} = \frac{1}{2\hbar^2}\int_{-\infty}^{\infty} d\tau \overline{\{\langle\alpha|H_1(t)|\alpha\rangle - \langle\beta|H_1(t)|\beta\rangle\}\{\langle\alpha|H_1(t-\tau)|\alpha\rangle\langle\beta|H_1(t-\tau)|\beta\rangle\}} \quad ,$$

and

$$\Gamma'_{\alpha\beta} = \frac{1}{2\hbar^2}\int_{-\infty}^{\infty} d\tau \Bigg\{\sum_{\gamma\neq\alpha}\overline{\langle\alpha|H_1(t)|\gamma\rangle\langle\gamma|H_1(t-\tau|)|\alpha\rangle}\exp(i\omega_{\alpha\gamma}\tau) \tag{4}$$

$$+\sum_{\gamma\neq\beta}\overline{\langle\beta|H_1(t-\tau)|\gamma\rangle\langle\gamma|H_1(t)|\beta\rangle}\exp(i\omega_{\alpha\gamma}\tau)\Bigg\}. \tag{5}$$

The first term is referred to as the adiabatic term which is a special characteristic of transverse relaxation. It does not contribute to the longitudinal relaxation. The second term (nonadiabatic term) is related to the lifetimes $t_\alpha$ and $t_\beta$ of states $|\alpha\rangle$ and $|\beta\rangle$ through

$$\frac{1}{t_\alpha} = \frac{1}{\hbar^2}\int_{-\infty}^{\infty} d\tau \sum_{\gamma\neq\alpha}\langle\alpha|H_1(t)|\gamma\rangle\langle\gamma|H_1(t-\tau)|\alpha\rangle\exp(i\omega_{\alpha\gamma}\tau) \quad , \tag{6}$$

$$\frac{1}{t_\beta} = \frac{1}{\hbar^2}\int_{-\infty}^{\infty} d\tau \sum_{\gamma\neq\beta}\langle\beta|H_1(t)|\gamma\rangle\langle\gamma|H_1(t-\tau)|\beta\rangle\exp(i\omega_{\beta\gamma}\tau) \quad , \tag{7}$$

and

$$\Gamma'_{\alpha\beta} = \tfrac{1}{2}(1/t_\alpha + 1/t_\beta) \quad . \tag{8}$$

The nonadiabatic term contributes to the linewidth due to the finite lifetime of states $|\alpha\rangle$ and $|\beta\rangle$ by the longitudinal relaxation mechanisms

### B. Relaxation by paramagnetic impurity

The effect of the NMR line broadening by the addition of small quantities of paramagnetic species to a sample was first observed by Bloch *et al.*[14] This effect was interpreted as a fluctuating electron–nuclear dipole–dipole interaction.[15] Even at small concentrations, this mechanism can be more important than intra- and internuclear dipolar interactions because the magnetic moment of an unpaired electron is of the order of $10^3$ times larger than the moment of a nucleus. It is predicted that the relaxation rate should be proportional to the concentration of the paramagnetic impurity and the square of the effective magnetic moment of the electron on the impurity.[15]

The dipole–dipole interaction between the unpaired electron and the methyl protons is given by

$$H_1(t) = \sum_{i=1,2,3}\hbar^2\gamma_I\gamma_S\left(\frac{\mathbf{I}_i\cdot\mathbf{S}}{r_i^3} - 3\frac{(\mathbf{I}_i\cdot\mathbf{r}_i)(\mathbf{S}\cdot\mathbf{r}_i)}{r_i^5}\right) \quad , \tag{9}$$

where $\gamma_I$ and $\gamma_S$ are the gyromagnetic ratios of proton and electron, respectively. The vector $\mathbf{r}_i$ defines the position of the proton as shown in Fig. 3. If the concen-

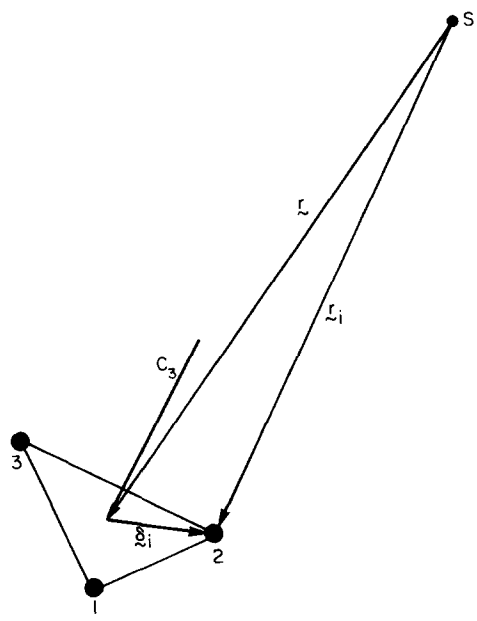


FIG. 3. Geometry of interacting methyl group and electron. $\mathbf{r}_i$ is the vector from the electron of the paramagnetic impurity to one of methyl protons. The vector $\mathbf{r}$ defines the position of the center of the triangle of the methyl protons with respect to the electron. $\delta_i$ is the vector from the center of the triangle to one of the protons.

tration is low, it is legitimate to expand the above expression in $\delta/r$. Using symmatry-adapted operators, one obtains[16]

$$H_1(t) = \sqrt{3}\hbar^2\gamma_I\gamma_S\left(\frac{\mathbf{I}_A\cdot\mathbf{S}}{r^3} - \frac{3(\mathbf{I}_A\cdot\mathbf{r})(\mathbf{S}\cdot\mathbf{r})}{r^5}\right) - \frac{3\hbar^2\gamma_I\gamma_S}{r^5}$$
$$\times \sum_{\mu=E^a,E^b}[(\mathbf{I}_\mu\cdot\sigma_{\bar{\mu}})(\mathbf{S}\cdot\mathbf{r}) + (\mathbf{I}_\mu\cdot\mathbf{r})(\mathbf{S}\cdot\sigma_{\bar{\mu}}) + (\mathbf{I}_\mu\cdot\mathbf{S})(\mathbf{r}\cdot\sigma_{\bar{\mu}})]$$
$$+ \frac{15\hbar^2\gamma_I\gamma_S}{r^7}\sum_{\mu=E^a,E^b}(\mathbf{I}_\mu\cdot\mathbf{r})(\mathbf{S}\cdot\mathbf{r})(\mathbf{r}\cdot\sigma_{\bar{\mu}}) \quad , \tag{10}$$

where

$$\mathbf{I}_\mu = \frac{1}{\sqrt{3}}(\mathbf{I}_1 + \lambda\mathbf{I}_2 + \lambda^*\mathbf{I}_3), \qquad \delta_{\bar{\mu}} = \frac{1}{\sqrt{3}}(\delta_1 + \lambda^*\delta_2 + \lambda\delta_3) \quad , \tag{11}$$

$\mu = A$, $E^a$, or $E^b$ for $\lambda = 1$, $\epsilon$ or $\epsilon^*$.

The first term in the above equation containing only $A$ symmetry operators connects states of the same irreducible representation of the $C_3$ symmetry group. The second and third terms containing $E^a$ and $E^b$ symmetry operators will violate the symmetry and cause symmetry breaking relaxation pathways.

Without loss of generality, the dipole–dipole interaction between the methyl protons and the unpaired electron can be expressed as a product of tensor operators[17,18]

$$H_1(t) = -\hbar\gamma_I\sum_{i=1,2,3}\mathbf{I}_i\cdot\mathbf{B}_i(t) = \sum_{\substack{m=0,\pm1\\ i=1,2,3}}(-1)^m V_i^{(m)}\mathcal{F}_i^{(m)}(t)$$
$$= \sum_{\substack{m=0,\pm1\\ \mu=A,E^a,E^b}}(-1)^m V_\mu^{(m)}\mathcal{F}_\mu^{(m)}(t) \quad , \tag{12}$$

where

$$V_i^{(0)} = I_{i,z},$$
$$V_i^{(1)} = -\frac{1}{\sqrt{2}}(V_{i,x} + iV_{i,y}) \text{ and } V_i^{(-1)} = \frac{1}{\sqrt{2}}(V_{i,x} - iV_{i,y}) \quad . \tag{13}$$

The symmetry-adapted form $V_\mu^{(m)}$ is related to $V_i^{(m)}$ by the same transformation as in Eq. (11). The fluctuating local field $\mathbf{B}_i(t)$ experienced by the proton spin $\mathbf{I}_i$ is produced by the unpaired electron.

There are two kinds of correlation functions involved in our discussion. These are autocorrelation functions $G_a(\tau)$ and cross-correlation function $G_c(\tau)$ which are given by

$$(-1)^m\overline{\mathcal{F}_i^{(-m)}(t)\mathcal{F}_i^{(n)}(t-\tau)} = \delta_{mn}G_a^{(m)}(\tau) \quad , \tag{14}$$

$$(-1)^m\overline{\mathcal{F}_i^{(-m)}(t)\mathcal{F}_j^{(n)}(t-\tau)} = \delta_{mn}G_c^{(m)}(\tau) \quad \text{for } i\neq j \quad . \tag{15}$$

One may express the correlation function in terms of symmetry of the molecule as

$$(-1)^m\overline{\mathcal{F}_\mu^{(-m)}(t)\mathcal{F}_{\mu'}^{(n)}(t-\tau)} = \delta_{mn}\delta_{\mu\mu'}G_\mu^{(m)}(\tau) \quad . \tag{16}$$

It can be shown that the symmetry-adapted correlation function is closely related to the autocorrelation function and cross-correlation function by

$$G_\mu^{(m)}(\tau) = \begin{cases} G_a^{(m)}(\tau) + 2G_c^{(m)}(\tau) & \text{if } \mu = A \\ G_a^{(m)}(\tau) - G_c^{(m)}(\tau) & \text{if } \mu = E^a, E^b \quad . \end{cases} \tag{17}$$

The transitions between states $(A_{1/2}, A_{-1/2})$, $(E^a_{1/2}, E^a_{-1/2})$, $(E^b_{1/2}, E^b_{-1/2})$ have the same frequency. The decay of the coherence for these degenerate transitions is in general nonexponential and complicated. The decay rates for the nondegenerate multiple quantum transitions are evaluated and given as follows:

$$\left.\begin{aligned} \hbar^2\Gamma_{14} &= \tfrac{3}{2}J_A^{(0)} + \tfrac{1}{2}J_A^{(1)} + J_{E^a}^{(1)} \quad , \\ \hbar^2\Gamma_{13} = \hbar^2\Gamma_{24} &= \tfrac{2}{3}J_A^{(0)} + \tfrac{5}{6}J_A^{(1)} + \tfrac{1}{3}J_{E^a}^{(0)} + \tfrac{2}{3}J_{E^a}^{(1)} \quad , \\ \hbar^2\Gamma_{12} = \hbar^2\Gamma_{34} &= \tfrac{1}{6}J_A^{(0)} + \tfrac{5}{6}J_A^{(1)} + \tfrac{1}{3}J_{E^a}^{(0)} + \tfrac{2}{3}J_{E^a}^{(1)} \quad . \end{aligned}\right\} \tag{18}$$

The spectral densities are related to Fourier transformations of correlation functions by

$$\left.\begin{aligned} J_A^{(0)} &= 2G_a^{(0)}(0)(1+2\xi) \quad , \\ J_A^{(1)} &= 2G_a^{(1)}(\omega_I)(1+2\xi) \quad , \\ J_{E^a}^{(0)} = J_{E^b}^{(0)} &= 2G_a^{(0)}(0)(1-\xi) \quad , \\ J_{E^a}^{(1)} = J_{E^b}^{(1)} &= 2G_a^{(1)}(\omega_I)(1-\xi) \quad , \end{aligned}\right\} \tag{19}$$

where

$$\xi = G_c^{(0)}/G_a^{(0)} = G_c^{(1)}/G_a^{(1)} \quad , \tag{20}$$

and $\omega_I$ is the Lamor frequency of the proton.

The asymmetry parameter (or correlation parameter) $\xi$ is a measure of the extent of the symmetry-breaking relaxation.

(1) Completely correlated fluctuation, $\xi = 1$. In this case each proton in the methyl group experiences the same field produced by the unpaired electron. It implies that the autocorrelation function and cross-correlation function be equal, i.e., $\xi = 1$. One readily obtains

$$\left.\begin{aligned} G_A^{(m)}(\tau) &= 3G_a^{(m)}(\tau) \quad , \\ G_{E^a}^{(m)}(\tau) &= G_{E^b}^{(m)}(\tau) = 0 \quad . \end{aligned}\right\} \tag{21}$$

The allowed relaxation channels are those transitions conserving symmetry.

(2) Completely uncorrelated fluctuation, $\xi = 0$. In this case each proton spin is relaxed independently by the electron. The inter-symmetry-crossing relaxation is allowed and the cross-correlation function vanishes; i.e.,

$$G_A^{(m)}(\tau) = G_{E^a}^{(m)}(\tau) = G_{E^b}^{(m)}(\tau) = G_a^{(m)}(\tau) \quad . \tag{22}$$

(3) General case. The ratios of the decay rates of multiple quantum coherences depend on the asymmetry parameter $\xi$ and the ratio of $G_a^{(0)}/G_a^{(1)}(\omega_I)$ which depends on the correlation time $\tau_c$ of the fluctuation and the Lamor frequencies $\omega_I$, $\omega_S$ of proton and electron. As evaluated in the Appendix, the correlation functions are given by

$$G_a^{(0)}(0) = \tfrac{1}{5}K^2\tau_c + \tfrac{3}{10}K^2\tau_c\frac{1}{1+\omega_s^2\tau_c^2} \quad , \tag{23}$$

$$G_a^{(1)}(\omega_I) = G_a^{(-1)}(\omega_I) = \tfrac{3}{20}K^2\tau_c\frac{1}{1+\omega_I^2\tau_c^2} + \tfrac{7}{20}K^2\tau_c\frac{1}{1+\omega_s^2\tau_c^2} \quad , \tag{24}$$

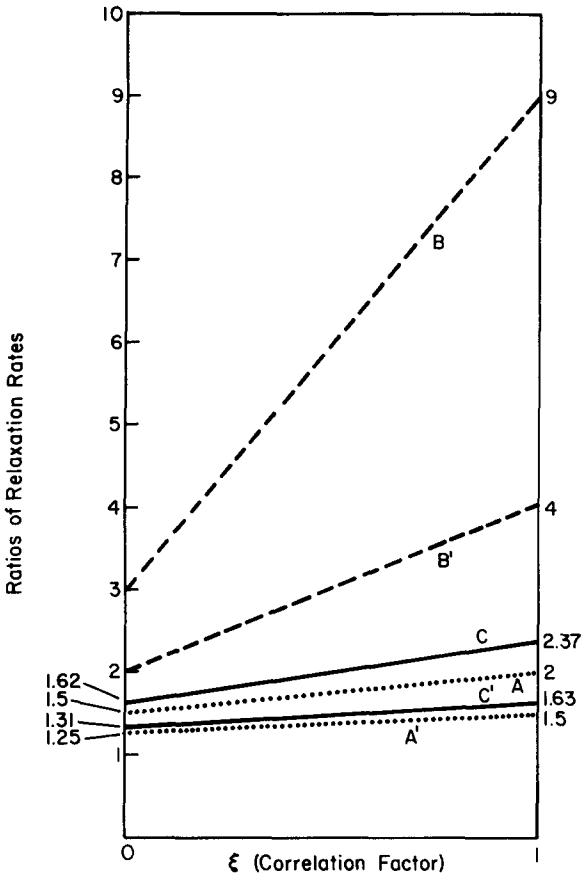


FIG. 4. The ratios of relaxation rates of double and triple quantum coherences to single quantum $\Gamma_{13}/\Gamma_{12}$ and $\Gamma_{14}/\Gamma_{12}$ depends on the correlation factor $\xi$ and the coreelation time $\tau_c$. Curves $A$ and $A'$ show the case of short correlation time limit, $\omega_s^2\tau_c^2 \ll 1$. Lines $B$ and $B'$ show the case of long correlation time limit, $\omega_I^2\tau_c^2 \gg 1$. The intermediate case, $\omega_I^2\tau_c^2 \ll 1$, $\omega_S^2\tau_c^2 \gg 1$, is shown by curves $C$ and $C'$.

where

$$K^2 = \left\langle \left( \frac{\hbar^2\gamma_I\gamma_S}{r^3} \right)^2 \right\rangle \quad .$$

The dependence of the decay rates on the concentration of paramagnetic impurity is through the average distance between electron and methyl proton.

The ratios of the relaxation rates (independent of the concentration of impurity in the experimental range) provide a measurement of the correlation time and the asymmetry parameter.

As an illustration of the sensitivity of the $n$-quantum relaxation to the fluctuation model, the ratios of the decay rates are illustrated for three extreme cases which are classified by the value of $\tau_c$.

(a) Short correlation time limit, $\omega_s^2\tau_c^2 \ll 1$.

The ratios of decay rates is given by

$$\frac{\Gamma_{14}}{\Gamma_{12}} = \frac{3(1+\xi)}{2+\xi} \quad , \qquad \frac{\Gamma_{13}}{\Gamma_{12}} = \frac{\frac{5}{2}+2\xi}{2+\xi} \quad . \tag{25}$$

Their dependence on $\xi$ are indicated by the two curves $A$ and $A'$ in Fig. 4.

(b) Long correlation time limit, $\omega_I^2\tau_c^2 \gg 1$.

In this case, one has

$$\frac{\Gamma_{14}}{\Gamma_{12}} = 3+6\xi, \quad \frac{\Gamma_{13}}{\Gamma_{12}} = 2+2\xi \quad . \tag{26}$$

The dependence of the ratios on $\xi$ are indicated by the two curves $B$ and $B'$ in Fig. 4.

(c) Intermediate case, $\omega_I^2\tau_c^2 \ll 1$, $\omega_s^2\tau_c^2 \gg 1$.

The ratios are given by

$$\frac{\Gamma_{14}}{\Gamma_{12}} = \frac{21+24\xi}{13+6\xi} \quad , \qquad \frac{\Gamma_{13}}{12} = \frac{17+14\xi}{13+6\xi} \quad . \tag{27}$$

Their dependence on $\xi$ are indicated by the two curves $C$ and $C'$ in Fig. 4.

## IV. EXPERIMENTAL RESULTS AND DISCUSSION

### A. Samples and spectrometer

Experiments were done in a field of 42.5 kG provided by Bruker superconducting solenoid. The corresponding operating frequency for protons is 185 MHz. The pulsed rf power of 200 W generated by a tuned transmitter produced a rotating field of 20 G in a solenoidal coil of 8 mm in diameter. Samples of acetonitrile (−12% in mole) dissolved in EBBA ($p$-ethoxy-benzylidine $n$-butylaniline) with different concentrations of di-$t$-butyl-nitroxide (DTBN) radical were observed over a range of temperature 21.5–23.0 °C. The temperature was controlled by a feedback system within ±0.1 °C. The change of the observed dipolar splitting by temperature fluctuation causes line broadening by an amount less than a few hertz.

### B. Pulse sequence

Multiple quantum transitions were observed by TPPI–Echo method.[6] The line broadening by field inhomogeneity (~1 ppm) was removed by the echo pulse[19] during the evolution period of multiple quantum coherences as shown in Fig. 5. An artificial frequency offset was created by the increment of the phase of the first two 90° pulses relative to that of the third 90° pulse. This

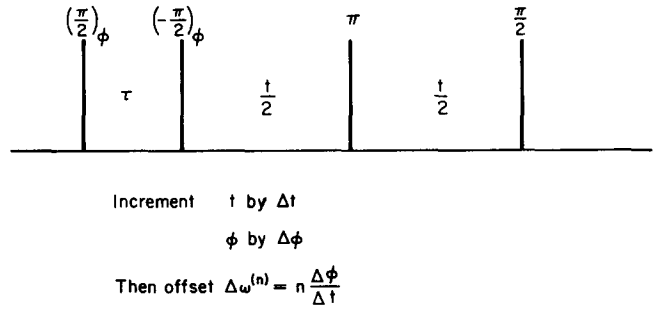


FIG. 5. The TPPI–echo pulse sequence is used to remove inhomogeneous line broadening and to restore the frequency offset by the time proportional phase increments. The artificial frequency offset is merely the rate of phase increment. The time during the period of preparation and mixing is set to be 250–500 μsec. The multiple quantum spectrum is obtained by Fourier transformation of the signal in time domain of $t$.

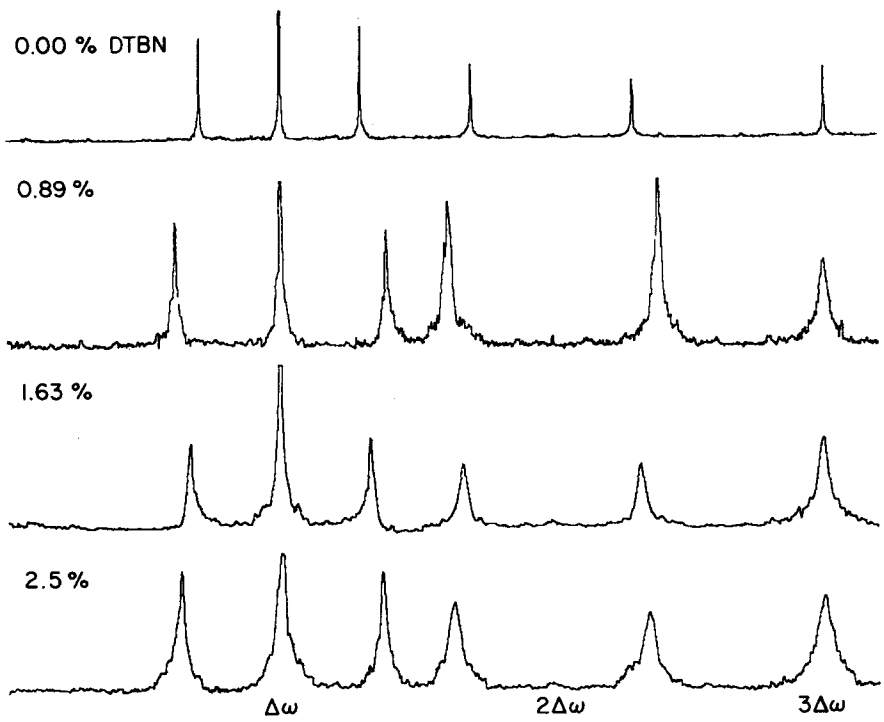


FIG. 6. The relaxation rates of multiple quantum coherence depend on the concentration of the paramagnetic imputiy. Shown are illustrative multiple quantum spectra with different concentrations of DTBN in mole% The frequency offset $\Delta\omega/2\pi$ is 7.8125 kHz.

capitalizes on the fact that when the rf phase is incremented by $\phi$ the $n$-quantum transitions "see" this as $n\phi$.[3,5-7].

### C. Spectra and results

The linewidths of multiple quantum transitions for a given concentration of DTBN were measured by taking averages of the particular linewidth of spectra obtained with various $\tau$ ranging from 250 to 500 $\mu$sec. Four typical spectra with different concentrations of DTBN are shown in Fig. 6.

The full widths at half height of each transitions, related to relaxation rate by $\Gamma/\pi$, were found to vary linearly with respect to the concentration of the impurity as shown in Fig. 7. Their relations are given by linear fits:

$$\Gamma_{12} = \Gamma_{34} = (336 \pm 5)\,[C]\ \text{sec}^{-1}\ ,$$

$$\Gamma_{13} = \Gamma_{24} = (565 \pm 10)\,[C]\ \text{sec}^{-1}\ ,$$

$$\Gamma_{14} = (850 \pm 90)\,[C]\ \text{sec}^{-1}\ ,$$

where [C] is the concentration of DTBN in mole%.

The ratios of the decay rates $\Gamma_{14}/\Gamma_{12}$ and $\Gamma_{13}/\Gamma_{12}$ are then

$$\Gamma_{13}/\Gamma_{12} = 1.68 \pm 0.02,$$

$$\Gamma_{14}/\Gamma_{12} = 2.53 \pm 0.15\ .$$

### D. Discussion

We now compare the various models of correlation time $\tau_c$ and correlation parameter $\xi$ (Fig. 4) with these data. The model with the condition $\omega_s^2 \tau_c^2 \ll 1$ is completely ruled out since it predicts (Curves $A$ and $A'$ in Fig. 4)

$$\Gamma_{13}/\Gamma_{12} = 1.25\text{–}1.50 \qquad \text{for } \xi = 0\text{–}1\ .$$

$$\Gamma_{1A}/\Gamma_{12} = 1.50\text{–}2.00$$

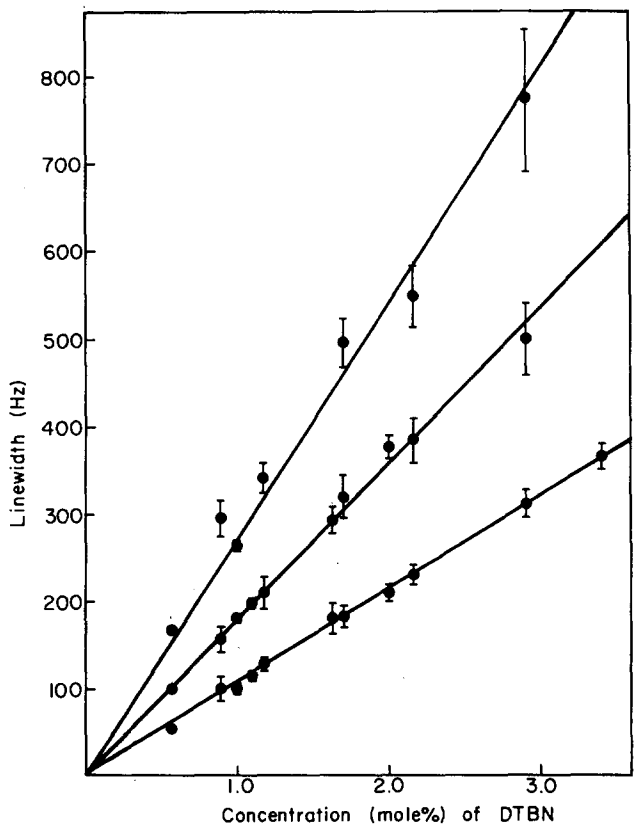


FIG. 7. The linewidth of multiple quantum transitions is linearly proportional to the concentration of DTBN. The ratios of the relaxation rates can be determined accurately by measuring the ratios of the slope.

Similarily, $\omega_I^2 \tau_c^2 \gg 1$ is not possible since it predicts (Curves $B$ and $B'$ in Fig. 4)

$$\Gamma_{13}/\Gamma_{12} = 2.0\text{–}4.0 \quad \text{for } \xi = 0\text{–}1 \ .$$
$$\Gamma_{14}/\Gamma_{12} = 3.0\text{–}9.0$$

Looking at Curves $C$ and $C'$ in Fig. 4, we see that the data can be fit quite well with the assumption that $\omega_s^2 \tau_c^2 \gg 1$ and $\omega_I^2 \tau_c^2 \ll 1$ with $\xi = 1$. This predicts

$$\Gamma_{13}/\Gamma_{12} = 1.63 \quad \xi = 1 \ .$$
$$\Gamma_{14}/\Gamma_{13} = 2.37$$

The fit can be made very good by keeping $\xi = 1$ but with $y = (1 + \omega_I^2 \tau_c^2)^{-1} = 0.91 \pm 0.04$. With these values we find $\tau_c = (2.7 \pm 0.6) \times 10^{-10}$ sec.

The conclusion that $\xi = 1$, i.e., that there is complete correlation in the fluctuation is not unreasonable, since $\tau_c \sim 10^{-10}$ sec whereas the rotation time for the $CH_3$ group (permuting the proton positions) is of the order of $10^{-12}$ sec. In addition, the average distance between electron spin and the methyl protons is much larger than the dimensions of the methyl group. Simple geometric calculations (using $\delta/\gamma$) predict that the extent of symmetry breaking transitions should be less than 1%. Thus we see that indeed the measurement of $n$-quantum relaxation gives a very sensitive measure of correlation and correlation times.

### E. Summary and comments

In a system of strongly coupled spins, it has been shown that the longitudinal and transverse relaxation to normal single quantum transitions usually provides information about internuclear correlation functions. However, they alone are not adequate to determine the relaxation mechanism which is characterized by a number of auto- and cross-correlation functions. The advantages of using multiple quantum spectroscopy to study relaxation effect have been illustrated by the system of oriented actionotrile in a liquid crystal matrix with paramagnetic impurities.

It is estimated that the broadening of linewidths by paramagnetic impurity becomes dominant over those by intra- and interproton relaxation if the molar concentration of paramagnetic impurity is larger than 0.01%. The estimated contribution of line broadening by symmetry-breaking channels is rather small (<1%), even with molar concentrations as high as 35%.

The presence of the echo pulse during the period of the evolution of multiple quantum coherences reverses the magnetic quantum number $m$ and changes density matrix element $\rho_{\alpha\beta}$ into $\rho_{\alpha'\beta'}$, where $|\alpha'\rangle$, $|\beta'\rangle$ are mirror-imaged states of $|\alpha\rangle$ and $|\beta\rangle$ by reversing $m$. However, the associated dipolar splitting and relaxation rates remain unchanged.

It is interesting to point out some features of the case of completely correlated fluctuations. The adiabatic term of the relaxation rate originated from the elastic scattering (energy-converging) processes can be written as

$$\Gamma_{\alpha\beta}^{(0)} = \frac{1}{2\hbar^2} J_A^{(0)}(0)(m_\alpha - m_\beta)^2 \ .$$

It has a simple quadratic dependence of the decay rates on the number of quanta. In the case of long correlation time limit ($\omega_I^2 \tau_c^2 \gg 1$) the nonadiabatic contribution due to inelastic scattering processes becomes negligible. The linewidth of $n$-quantum coherence depends on $N$ quadratically. It is a general property of the case of completely correlated fluctuations without referring particularly to the system of methyl protons. As the correlation time becomes shorter, the nonadiabatic contribution becomes as important as the adiabatic term. The nonadiabatic term can be found by evaluation of the lifetimes of the associated states.

The expression of the adiabatic term in the case of completely uncorrelated fluctuations is generally complicated. However, there is a simple relation if either state $|\alpha\rangle$ or $|\beta\rangle$ is the highest or lowest state. In this case, the adiabatic term linearly depends on the number of quanta of the multiple quantum coherence, i.e.,

$$\Gamma_{\alpha\beta}^{(0)} = \frac{1}{2\hbar^2} J^{(0)}(0) |m_\alpha - m_\beta| \ .$$

For a system of $N$ coupled spins, the nonadiabatic term has a simple form in the case of completely uncorrelated fluctuations:

$$\Gamma'_{\alpha\beta} = \frac{1}{2\hbar^2} J^{(1)}(\omega_I) N \ .$$

It is due to the fact that each spin relaxes independently and contributes to the decay rate equally.

There is only one transition between the state with all spins up and the state with all spins down. The adiabatic term of its linewidth depends on the number of quanta quadratically in the case of completely correlated fluctuation and linearly in the case of completely uncorrelated fluctuations.

## ACKNOWLEDGMENTS

We would like to acknowledge the help of Mr. Sidney Wolfe in synthesis of the paramagnetic impurity and the liquid crystal. This work has been supported by the Division of Materials Sciences, Office of Basic Energy Sciences, U. S. Department of Energy under contract No. W7405-ENG-48.

## APPENDIX

The dipolar interaction between electron and proton is given by

$$H_1(t) = \frac{\hbar^2 \gamma_I \gamma_S}{r^3} [\mathbf{I} \cdot \mathbf{S} - 3(\mathbf{I} \cdot \mathbf{r})(\mathbf{S} \cdot \mathbf{r})]$$
$$= K \sum_{m=2}^{2} (-1)^m V^{(m)} \mathcal{F}^{(-m)}(t) \ ,$$

where

$$V^{(0)} = I_z, \quad V^{(1)} = -\frac{1}{\sqrt{2}} I_+, \quad V^{(-1)} = \frac{1}{\sqrt{2}} I_-, \quad K = \frac{\hbar^2 \gamma_I \gamma_S}{r^3} \ ,$$

and

and

$$f^{(0)}(t) = F_0(t)S_z(t) + F_1(t)S_+(t) + F_{-1}(t)S_-(t) ,$$

$$f^{(1)}(t) = \sqrt{2}\,(-\tfrac{1}{4}F_0(t)S_-(t) + F_1(t)S_z(t) + F_2(t)S_+(t)) ,$$

$$f^{(-1)}(t) = -(f^{(1)}(t))^+ ,$$

$$f^{(m)}(t-\tau) = e^{iH_0\tau} f^{(m)}(t) e^{-iH_0\tau} .$$

Here the spherical harmonic functions of second rank $F_m(t)$ are defined as[20]

$$F_0 = 1 - 3\ \cos^2\theta ,$$

$$F_1 = -\tfrac{3}{2}\sin\theta\cos\theta\, e^{i\phi} ,$$

$$F_2 = -\tfrac{3}{4}\sin^2\theta\, e^{2i\phi} ,$$

$$F_{-m} = F_m^* .$$

The correlation function in the frequency domain is given by

$$G_a^{(m)}(m\omega_I) = \frac{1}{2}\int_{-\infty}^{\infty} (-1)^m \overline{d\tau f^{(-m)}(t) f^{(m)}(t-\tau)} \exp(-im\omega_I\tau) .$$

One obtains

$$G_a^{(0)}(0) = \tfrac{1}{5}K^2\tau_c + \tfrac{3}{10}K^2\tau_c \frac{1}{1+\omega_s^2\tau_c^2} ,$$

$$G_a^{(1)}(\omega_1) = G_a^{(-1)}(\omega_1) = \tfrac{3}{20}K^2\tau_c \frac{1}{1+\omega_I^2\tau_c^2} + \frac{7}{20}K^2\tau_c \frac{1}{1+\omega_s^2\tau_c^2} .$$


[1] H. Hatanaka and T. Hashi, J. Phys. Soc. Jpn. **39**, 835 (1975); H. Hatanaka, T. Terao, and T. Hashi, J. Phys. Soc. Jpn. **39**, 1139 (1975).

[2] W. P. Aue, E. Bartholdi, and R. R. Ernst, J. Chem. Phys. **64**, 2229 (1976).

[3] S. Vega, T. W. Shattuck, and A. Pines, Phys. Rev. Lett. **37**, 43 (1976); S. Vega and A. Pines, J. Chem. Phys. **66**, 5624 (1977); A. Pines *et al.*, *Magnetic Resonance in Condensed Matter-Recent Developments*, Proceedings of the IVth Ampere School, Pula, edited by R. Blinc and G. Lahajnar (University of Ljubljana, 1977), p. 128–179.

[4] M. E. Stoll, A. J. Vega, and R. W. Vaughan, J. Chem. Phys. **67**, 2029 (1977).

[5] A. Pines, D. Wemmer, J. Tang, and S. Sinton, Bull. Am. Phys. Soc. **23**, 21 (1978); D. Wemmer, Ph. D. thesis, Berkeley, 1978.

[6] G. Drobny, A. Pines, S. Sinton, D. Weitekamp, and D. Wemmer, Faraday Symposium, University of London, 1978 (in press).

[7] A. Wokaun and R. R. Ernst, Mol. Phys. **36**, 317 (1978); A. Wokaun and R. R. Ernst, Chem. Phys. Lett. **52**, 407 (1977).

[8] R. Poupko, R. L. Vold, and R. R. Vold, J. Magn. Reson. **34**, 67 (1979); G. Bodenhausen, R. L. Vold, and R. R. Vold, J. Magn. Reson. (in press).

[9] L. G. Werbelow and D. M. Grant, Adv. Magn. Reson. **9**, 180 (1977).

[10] J. P. Jacobson, H. K. Bildsøe, and K. Schaumburg, J. Magn. Reson. **23**, 153 (1976).

[11] S. Emid, R. J. Baarda, J. Smidt, and R. A. Wind, Physica (Utrecht) B **93**, 327 (1978).

[12] A. G. Redfield, IBM J. Res. Dev. **1**, 19 (1957); A. G. Redfield, Adv. Magn. Reson. **4**, 87 (1970).

[13] A. Abragam, *The Principles of Nuclear Magnetism* (Oxford U. P., London, 1961).

[14] F. Bloch, W. W. Hansen, and M. E. Packard, Phys. Rev. **70**, 474 (1946).

[15] N. Bloembergen, E. M. Purcell, and R. V. Pound, Phys. Rev. **73**, 679 (1948).

[16] S. Clough and T. Hobson, J. Phys. C **7**, 3387 (1974).

[17] M. Tinkham, *Group Theory and Quantum Mechanics* (McGraw-Hill, New York, 1964).

[18] R. A. Hoffman, Adv. Magn. Reson. **4**, 87 (1970).

[19] E. L. Hahn, Phys. Rev. **80**, 580 (1959).

[20] L. Solomon, Phys. Rev. **99**, 559 (1955).